

NAG 9-189

JOHNSON  
GRAN  
7N-25-UR

Computer Simulation of Inverse Gas Chromatography  
Elution Behavior: Comparison with Experiment.

252370

138

Paul Hattam, Qiangguo Du<sup>1</sup> and Petr Munk

Department of Chemistry and Center for Polymer  
Research, The University of Texas at Austin  
Austin, Texas 78712

(NASA-CR-186150) COMPUTER SIMULATION OF  
INVERSE GAS CHROMATOGRAPHY ELUTION BEHAVIOR:  
COMPARISON WITH EXPERIMENT (Texas Univ.)

N90-70344

13 p

Unclass

00/25 0252390

In order to facilitate the analysis of the shape and position of elution curves in inverse gas chromatography, such curves were generated in a computer for many well-defined situations. The effects of diffusion in the gas phase, of slow diffusion in the polymer phase (compared to an instantaneous equilibration of the probe), and of surface adsorption (Langmuir type) were simulated. A set of evaluation guidelines was established and was applied to several model experiments.

The use of inverse gas chromatography (IGC) to study the properties of polymers has greatly increased in recent years (1,2). The shape and position of the elution peak contain information about all processes that occur in the column: diffusion of the probe in the gas and the polymer phases, partitioning between phases, and adsorption on the surface of the polymer and the support. Traditional IGC experiments aim at obtaining symmetrical peaks, which can be analyzed using the van Deemter (3) or moments method (4). However, the behavior of the polymer-probe system is also reflected in the asymmetry of the peak and its tail. A method that could be used to analyze a peak of any shape, allowing elucidation of all the processes on the column, would be of great use.

It is difficult to separate the effects of the various processes contributing to the shape and position of an experimental elution peak because, in most instances, it is not obvious which factors are at play in any particular experiment. Hence, it is useful to analyze various models of chromatographic processes theoretically and follow their effect on the elution peak. However, the differential equations describing these models

1. Permanent Address: Materials Science Institute of Fudan University, Shanghai, People's Republic of China.

may be solved analytically only for the simplest models. It is possible to cast these differential equations in the form of difference equations and follow the development of the system by a computer. This paper reports the results of our computer simulations for some simple systems and compares the results with appropriate experimental data.

### Traditional Analysis of Elution Curves

The commonly used method of analysis postulates that ideal elution curves are symmetrical and Gaussian. The time at the position of the peak maximum,  $t_R$ , is a measure of the distribution coefficient of the probe between the stationary and mobile phases; peak spreading is expressed by the height equivalent to one theoretical plate  $H$ , which may be written as  $H = L/N$ ,  $N$  being the number of theoretical plates and  $L$  the column length. Furthermore we may write

$$N_P = (t_R/W_{1/2})^2 8 \ln 2 \quad (1)$$

$W_{1/2}$  denotes the peak width at half height; and subscript  $P$  denotes a parameter obtained from peak dimensions. The extended (5) van Deemter equation (3) may be written in a general form as

$$H = A + 2\gamma D_G/u + (C_G + C_L)u \quad (2)$$

$A$  is an eddy diffusion term to account for the various pathways in packed columns which lead to peak spreading;  $\gamma$  is the tortuosity factor which often has a value close to unity;  $u$  is the linear velocity of the carrier gas; terms  $C_G$  and  $C_L$  account for radial diffusion in the gas phase and the liquid phase respectively. We have found experimentally on packed columns that the  $C_G$  term is negligible (6). The expression for the  $C_L$  term may be written as

$$C_L = J d_f^2 k' / (1 + k')^2 D_L \quad (3)$$

$D_G$  and  $D_L$  are the diffusion coefficients of the probe in the two phases.  $J$  is a numerical constant and is equal to  $8/\pi^2$  according to van Deemter (3), and equal to  $2/3$ , according to Giddings (7).  $d_f$  is the thickness of the polymer layer.

For the traditional model, the elution time at the peak maximum,  $t_R$ , is related to the capacity factor  $k'$  and partition coefficient  $K$  by

$$k' = K V_L/V_G \quad (4)$$

$$t_R = t_0(1 + k') = t_0(1 + K V_L/V_G) \quad (5)$$

Here  $t_0$  is the elution time of the marker (ideal, non-retained probe);  $V_L$  and  $V_G$  are the volumes of the two phases within the column.

Another method of analysis of elution peaks is based on the statistical moments of the curve and was first proposed by McQuarrie (8). The first moment,  $F_M$ , is the center of gravity of

the peak; it is equal to  $t_R$  for a hypothetical symmetrical peak. The second central statistical moment,  $S_M$ , is equal to the peak variance ( $\sigma^2$ ); it is related to  $H$  as

$$H_M = L/N = L \sigma^2 / t_R^2 = L S_M / t_R^2 \quad (6)$$

The subscript M refers to the method of moments. The method of moments is applicable to all chromatographic systems characterized by a linear partition isotherm (that is, for  $K = \text{constant}$ ) irrespective of diffusion processes deforming the elution peak.

When the partition isotherm is nonlinear (typically when surface adsorption is involved), the elution peaks exhibit long tails. Tailing is also caused by slow diffusion of the probe in the polymer and by technical artifacts: mixing in the injection chamber, etc.

### Computer Simulation

Diffusion of the probe in the gas and polymer phases, and adsorption on the support and on the polymer surface (both types of adsorption have nonlinear isotherms), simultaneously play an important role in IGC experiments and must be accounted for properly. An extensive computational program is planned to simulate the individual processes and to assess their influence on chromatographic behavior. In a recent paper, simulated behavior of three types of system was described (9). In the simplest case, only diffusion in the gas phase was operative. This case corresponds to elution of an ideal marker. Simultaneous effects of gaseous diffusion and partitioning of the probe between the phases, were simulated next, assuming an instantaneous equilibrium between the phases. This case corresponds to IGC using a low molecular weight stationary phase or a polymer well above its glass transition temperature. Simulation of the partition of the probe combined with its slow transport in the polymer phase and with gaseous diffusion was also performed.

It is convenient in dealing with the computer simulation to minimize the number of input variables governing the chromatographic processes. We were able to do this using just three characteristic numbers:  $Z_p$  for the partition of the probe at equilibrium,  $Z_g$  for the diffusion in the gas phase, and  $Z_f$  governing the diffusion of the probe in the polymer phase (it vanishes when the probe equilibrates instantly). These quantities are defined as

$$Z_p \equiv k' \equiv K V_L / V_G \quad (7)$$

$$Z_g \equiv D_g / uL \quad (8)$$

$$Z_f \equiv u d_f^2 / D_1 L \quad (9)$$

Should one wish, these variables can easily be converted back to their expanded form through the definitions given in Equations 7 - 9. Our measure of peak asymmetry is the ratio of half widths,  $R_2$ , (easily accessible experimentally); it is defined as a ratio of the

front half of  $W_2$  to its back half. For symmetrical peaks  $R_{1/2} = 1$ . Traditional analyses of elution peaks (Equations 2-6) in the present notation are

$$t_R = t_M = (1 + Z_p)t_0 \quad (10)$$

$$H_p = H_M = 2Zg + ZfZ_p/(1 + Z_p)^2 \quad (11)$$

We have simulated elution curves for many combinations of the characteristic numbers. The details of the simulation procedure were described elsewhere (9). Here we present only the main results of the simulations:

1. Elution peaks were always asymmetric, even for simple gaseous diffusion and no interaction with the polymer. The  $R_{1/2}$  values were well correlated by the following expression:

$$R_{1/2} = 1 - (1.664(Zg)^{1/2} + 1.225Zg) \quad (12)$$

This relation was also valid for interacting probes so long as the equilibration was instantaneous.

2. The elution time  $t_R$  was always shorter than required by Equation 10. For instantaneous equilibrium, the correlation yielded

$$t_R/t_0 = (1+Z_p)(1 - 2.77 Zg) \quad (13)$$

In this expression,  $t_0$  is the elution time of a hypothetical marker with vanishing values of  $D_g$  and hence  $Zg$ , which would travel through the column as a Dirac delta function.

3. When the liquid diffusion was slow (large values of  $Zf$ ), the probe eluted together with marker (that is,  $t_R/t_0 = 1$ ) and the interaction with the polymer was manifested only by a long tail on the elution peak.

4. When the ratio  $Zf/Z_p$  was less than approximately 0.5, then a pseudo-equilibrium was achieved, (the probe distributed itself between the phases in a more or less equilibrium manner at least near the end of the column), and  $t_R$  was given approximately as

$$t_R/t_0 = (1+Z_p)(1-2.77Zg) - 0.482Zf(1+0.68Zf/Z_p) \quad (14)$$

5. Asymmetry of the elution peak  $R_{1/2}$  and the value of  $H_p$  for slowly diffusing probes depended on the ratio  $Zf/Z_p$ . In the pseudo-equilibrium case ( $Zf/Z_p < 0.5$ ), the asymmetry was moderate and  $H_p$  was approximated by

$$H_p/L = 2Zg + 0.7 Zf Z_p/(1 + Z_p)^2 + 0.965 [ Zf Z_p/(1 + Z_p)^2 ]^2 \quad (15)$$

This relation is close to the van Deemter relation, Equation 10,

so long as  $Z_f Z_p / (1 + Z_p)^2$  is not too large. When the ratio  $Z_f / Z_p$  is close to unity,  $R_i$  is small and  $H_p$  is very difficult to correlate with the basic parameters. Finally, when  $Z_f / Z_p > 2$ , the  $H_p$  value approaches the marker-like value of  $2Z_g$  and the asymmetry decreases again.

6. The simulation results agreed fully with predictions of the moments method; both  $F_M$  and  $H_M$  were described by Equations 10 and 11. This was true even in the marker-like region, where the probes eluted essentially at  $t_R = t_0$  and the retention was manifested only as a long low tail.

The second simulation project was aimed at describing experiments in which retention results from surface adsorption characterized by a Langmuir-type isotherm. In this simulation, the characteristic parameters are  $Z_g$ ,  $Z_p$ ,  $Z_s$ , and  $R_i$ .  $Z_s$  is the distribution coefficient between the surface and the carrier gas at vanishing surface coverage.  $R_i$  is defined as the ratio  $R_i = M_{inj} / M_{tot}$  where  $M_{inj}$  is the mass of the probe injected and  $M_{tot}$  is the mass of the probe which would fully saturate the adsorbing surface. The surface simulation work shows that at infinite dilution

$$t_R / t_0 = (1 + Z_s + Z_p)(1 - 2.77Z_g) \quad (16)$$

$$F_M / t_0 = (1 + Z_s + Z_p) \quad (17)$$

With an increase in the amount injected (increasing  $R_i$ ) both  $t_R / t_0$  and  $F_M / t_0$  decrease;  $t_R$  decreasing more rapidly than  $F_M$ . At injected amounts greater than the surface capacity of the column

$$t_R / t_0 = (1 + Z_p)(1 - 2.77Z_g) \quad (18)$$

$$F_M / t_0 = (1 + Z_p) \quad (19)$$

that is, the surface effect becomes negligible. Figure 1 illustrates results obtained from the surface simulation for the dependence of  $t_R / t_0$  and  $F_M / t_0$  on  $\log_{10} M_{inj}$  ( $M_{tot} = 1$ ) for several values of  $Z_s$  with  $Z_p = 0$ .

### Materials and Methods

The experimental data presented in this paper represent typical data from chromatographic experiments that were performed during various IGC projects. The signal from the FID detector of the chromatograph was registered on an HP 3478A digital voltmeter and recorded by a microcomputer. The computer and voltmeter interfacing was performed by a GPIB interfacing board (National Instruments). Data acquisition in this manner allowed a reproducibility of approximately  $\pm 0.1$  s in retention time. Typical columns were 150 cm long and 6.35 mm O.D., and contained 60 to 80 mesh Chromosorb-W (acid washed and treated with dimethyl-dichloro-silane) either uncoated or coated with 7% (by weight) of polymer.

### Comparison of Simulation and Experiment

Demonstration of Instant Equilibration ( $Z_f = 0$ ). Data were gathered for several n-alkanes at various gas flow rates and column temperature of 100°C using a column coated with poly-isobutylene (PIB). Under these conditions PIB is far above its glass transition temperature ( $T_g$ ) and equilibration of probe and polymer is expected to be instantaneous.

For instantaneous equilibration, the simulation predicts that  $F_M$  is as predicted by theory, Equation 10, and  $t_R$  is given by equation 13. Thus  $t_R$  should be slightly less than  $F_M$  due to the gaseous diffusion coefficient. Table I shows the experimental values of  $t_R$  and  $F_M$  at several flow rates.

Table I. Flow rate dependence of  $t_R$  and  $F_M$  determined at 100°C for several n-alkanes on a poly-isobutylene column.

Probe	8 mL/min		16 mL/min		24 mL/min	
	$t_R$	$F_M$	$t_R$	$F_M$	$t_R$	$F_M$
C1	176.736	178.289	91.400	91.929	64.700	64.990
C5	215.807	219.211	110.932	111.689	78.680	79.277
C6	258.432	259.945	133.056	133.880	94.213	94.838
C7	346.817	348.676	178.822	179.847	126.335	127.114
C8	527.889	529.752	271.797	272.727	192.487	193.384

The difference between  $t_R$  and  $F_M$  is less than 1%, which is reasonable for the expected magnitude of  $Z_g$ . Two points indicate the system is in equilibrium. First, there is close agreement between  $t_R$  and  $F_M$ . Second,  $R_{1/2}$ , the width ratios for the probes measured under identical conditions for a coated and an uncoated column are essentially the same, see Table II.

Table II. The width ratio,  $R_{1/2}$ , obtained for several n-alkanes on an uncoated column and on a PIB column at 40°C and 100°C at a flow rate of 16 mL/min.

Probe	$R_{1/2}$ Chrom. W 40°C	$R_{1/2}$ Chrom. W 100°C	$R_{1/2}$ PIB 40°C	$R_{1/2}$ PIB 100°C
C1	0.951	0.942	0.949	0.946
C2	0.921	0.961	0.739	0.951
C3	0.918	0.963	0.796	0.923
C4	0.895	0.936	0.845	0.942
C5	0.817	0.942	0.888	0.946

By reducing the  $t_R$  of the probe by  $t_R$  of the marker ( $t'_R$ ), and reducing the  $F_M$  of the probe by  $F_M$  of the marker ( $F'_M$ ),  $1+Z_p$  for the probes is obtained. (Reduction in this manner accounts for part of the small error in  $t_R$  because of the effect of  $Z_g$ .) The reduced values ( $1+Z_p$ ) are shown in Table III. There is excellent

agreement between the values calculated from either  $t_R$  or  $F_M$ . In addition, the values are independent of flow rate, as is expected for instantaneous equilibration.

Table III. Reduced values of  $t_R$  and  $F_M$  determined for several n-alkanes at 100°C on a PIB column.

Probe	8 mL/min		16 mL/min		24 mL/min	
	$t_R/t'_M$	$F_M/F'_M$	$t_R/t'_R$	$F_M/F'_M$	$t_R/t'_R$	$F_M/F'_M$
C5	1.220	1.229	1.215	1.215	1.216	1.219
C6	1.461	1.457	1.458	1.456	1.455	1.458
C7	1.961	1.954	1.959	1.956	1.954	1.955
C8	2.985	2.970	2.978	2.966	2.974	2.973

Demonstration of Non-equilibrium ( $Z_f/Z_p < 0.5$ ). Data were gathered on the same PIB coated column as above at a temperature of 40°C. Under these conditions, diffusion of the probes into the polymer is not expected to be instantaneous. The simulation under these conditions predicts that  $F_M = (1 + Z_p)$  and  $t_R$  will be reduced by the effect of non-zero  $Z_f$ . The magnitude of the reduction is given by the second term of the right side of Equation 15. Since  $Z_f$  is dependent on flow rate, it is possible to estimate  $Z_f$  from the dependence of the peak width on the flow rate and hence, determine the size of the correction and compare it with experimental results. This comparison should be made bearing in mind that theoretically the simulation is applicable for capillary columns and not packed columns.

First, the true value of  $Z_p$  is determined by extrapolation of  $V_n/V_0$  to zero flow rate, where  $V_n$  is the net retention volume of the probe and  $V_0$  is the void volume of the column. These values are shown in Table IV. Second,  $u$ , the linear velocity of the carrier gas, is introduced into Equation 11 to give

$$u/N_p = 2Z_g u + (0.7Z_f Z_p / (1 + Z_p)^2) u \quad (20)$$

Substitution for  $Z_g$  and  $Z_f$  leads to

$$u/N_p = 2D_g/L + (0.7d_f^2 Z_p / D_1 L (1 + Z_p)^2) u^2 \quad (21)$$

Thus a plot of  $u/N_p$  versus  $u^2$  yields

$$\text{intercept} = 2D_g/L \quad (22)$$

$$\text{slope} = 0.7 d_f^2 Z_p / (1 + Z_p)^2 D_1 L \quad (23)$$

Rearrangement gives

$$Z_f = d_f^2 u / D_1 L = \text{slope} (1 + Z_p)^2 u / 0.7 Z_p \quad (24)$$

The correction predicted by Equation 15 is estimated and  $Z_p$  is adjusted.  $Z_p$  at zero flow rate, the experimental values and the corrected values for three flow rates, are given in Table IV.

Table IV.  $Z_p$  values of n-alkanes on a PIB column at 40°C; values at zero flow rate, at several flow rates, and at several flow rates corrected according to the simulation.

Flow (mL/min) Probe	$Z_p$	$Z_p$ from $t_R/t'_R$				$Z_p$ corrected		
	0	8	16	24		8	16	24
C5	0.872	0.832	0.800	0.777		0.842	0.822	0.810
C6	2.431	2.369	2.328	2.295		2.384	2.357	2.338
C7	6.700	6.600	6.546	6.511		6.681	6.678	6.692
C8	18.34	18.15	18.09	18.07		18.18	18.13	18.13

The predicted correction term is approximately three-fold less than would be required to adjust the experimental values to their value at zero flow rate. This difference is likely due to the range of polymer thickness in packed columns rather than the homogeneous coverage used in the simulation or for capillary columns. However, the first moment yields  $Z_p$  values that are in excellent agreement with  $Z_p$  values calculated at zero flow rate; Table V.

Table V. The  $Z_p$  values of several n-alkanes determined on a PIB column at 40°C; values at zero flow rate and values determined from the first moments.

Flow(mL/min) Probe	$Z_p$	$Z_p$ from $F_M/t'_R$			
	0	8	16	24	
C5	0.872	0.887	0.894	0.896	
C6	2.431	2.430	2.444	2.435	
C7	6.700	6.681	6.674	6.692	
C8	18.34	18.31	18.30	18.27	

This indicates that under these conditions,  $Z_p$  can be obtained from  $t_R$  only by extrapolating to zero flow rate, whereas  $F_M$  may be used regardless of the flow rate.

Determination of the Statistical Moments. The simulation confirmed that the method of moments offers a straight forward route to the data of interest for chromatographic experiments when isotherms are linear. However, in the past the experimental evaluation of the moments was imprecise. The statistical moments are extremely sensitive to tailing. Using the enhanced data acquisition techniques (signal to noise ratios of approximately  $5 \times 10^4$ ) the method of moments was re-examined. The presence of a long low tail on many of the elution peaks was observed on coated as well as uncoated columns. It was also noted that a long low tail was observed whenever the probe was injected in liquid form. When the injected amounts were the same, vapor injections greatly reduced tailing compared with liquid injections. The tailing is attributed to retention of the probe by the polymeric septum of the injection port. When the needle is inserted through the septum, the liquid at the tip of the needle is transferred to the



septum. The probe slowly eluting from the septum causes excessive tailing. Figure 2 illustrates the difference between the moments obtained from liquid injections and vapor injections. The use of vapor injections almost completely suppresses the effect of retention by the septum. The moments are extremely sensitive to tailing; the higher the moment, the greater the sensitivity. With small injections of vapors we have found that the first moment can be measured with confidence. Ideally a septum free system, should be used for the introduction of probes into the column if the higher moments are to be utilized. It is possible that headspace sampling gas chromatography could be used advantageously for this purpose (10).

Peak Asymmetry. The asymmetry of the elution curve reflects the various processes occurring in the column. To follow this asymmetry width ratio,  $R_z$ , defined earlier, was used. Although no quantitative relationship that can be applied with confidence experimentally was found via the simulation,  $R_z$  has proved to be a useful quantity. In the case of the simulation of surface adsorption at infinite dilution,  $R_z$  is close to unity. As injection size increases,  $R_z$  decreases until  $R_i = 1$ .  $R_z$  then increases again as the probe begins to elute in the marker-like region. It is hoped that in the future research will determine whether the dependence of  $R_z$  on probe concentration can be used in determining support surface area. In the simulation of bulk diffusion at instant equilibration  $R_z$  is close to unity. It decreases through the non-equilibrium region and again increases as marker-like behavior is observed. Though the processes that affect  $R_z$  in a particular experiment cannot be determined,  $R_z$  can be used as a guideline. For example, Table II shows  $R_z$  determined for several n-alkanes on the PIB column and on an uncoated column at 40°C and 100°C and a flow rate of 16 mL/min. At 100°C,  $R_z$  for probes on both uncoated and PIB columns are comparable and relatively large. This indicates that there is no anomalous behavior in the system. However the data for probes on the PIB column at 40°C show a considerably lower  $R_z$ , indicating that the system is not exhibiting instantaneous equilibration.

Acetone on Uncoated Support. Experiments in this section were performed on a column containing uncoated support at 40°C and 100°C and a flow rate of 16 mL/min. After treatment of the support with dimethyl-dichloro-silane, the resultant, so-called inert support, still contained a small number of active polar sites. These sites lead to adsorption of polar probes and thus the support contributes to the observed retention. One of the goals of this investigation was to facilitate the correction of retention data for the contribution of the support. The dependence of the acetone retention on the quantity injected (determined from peak area) was investigated. In the absence of polymer, any change in the retention with change of probe concentration was expected to be the result of surface adsorption. Also, by changing the temperature  $Z_s$  was effectively altered, (increasing temperature leading to a decrease of  $Z_s$ ), since the surface capacity of the column remained the same. Figure 1

illustrates the dependence of  $t_R/t_0$  and  $F_M/t_0$  on  $\log_{10} M_{inj}$  for the simulation at several  $Z_s$  values and with  $Z_p = 0$ . In Figure 3 we present the same dependence for the experimental data of acetone (in this instance the dependence is on  $\log_{10} A$ , peak area). While the simulation covers an extensive range of concentrations this may not be possible experimentally. Small injections are limited by the low detector signal (broad peaks magnifying this effect), while large injections are limited by non-linear detector response. However, even with the experimental range of concentrations covered, a comparison of the curves in Figures 1 and 3 is useful. It indicates that the results are in the region of moderately sized injections (for the number of active sites on the column). At 100°C  $Z_s$  is small, approximately 1 or 2, whereas at 40°C  $Z_s$  is greater by an order of magnitude. Although the precise value of  $Z_s$  cannot be determined as the injection size is far from the limit of infinite dilution, the value of  $F_M/t_0$  approaches unity with increasing amount of probe. This trend indicates that the retention is due to the surface of the support. Overall, the surface simulation and the experimental results compare favorably. Current work is focused on acquiring more data, both from experiment and from simulation. At this time it seems likely that in the future it will be possible to determine the capacity of the packing material for various probes. This will permit correction of probe retention data for the effect of the active surface sites on the support.

### Conclusions

The following conclusions were drawn from this research.

1. While the simulations do not predict exactly the results of experiment, they are extremely useful in predicting behavior trends.
2. The first moment can be used in the determination of characteristic numbers provided careful data acquisition and experimental procedure are followed. Use of higher moments should be handled with great caution.
3. Comparison of the elution time at peak maximum and the first moment is extremely informative as to what processes are affecting the retention of the probe.
4. By following the dependence of elution parameters on the amount of probe injected, it is possible to distinguish between surface adsorption and bulk adsorption of the probe.

### Acknowledgment

The authors are grateful for the financial support of the National Aeronautics and Space Administration, (Grant No. NAG9-189) and the National Science Foundation, (Grant No. DMR-8414575).

# Literature Cited.

1. Laub, J. R.; Pecsok, R. L. Physicochemical Applications of Gas Chromatography; Wiley: New York, 1978.
2. Aspler, J. S. In Pyrolysis and GC in Polymer Analysis; Chromatographic Science Series, Vol. 29: Liebman, S. A.; E. J. Levy Eds.; Dekker: New York, 1985. Chapter IX.
3. van Deemter, J. J.; Zuderweg, F. J.; Klinkenberg, A. Chem. Eng. Sci. 1956, 5, 271.
4. Vidal-Madjar, C.; Guiochon, G. J. Chromatogr. 1977, 61, 142.
5. Golay, M. J. E. Gas Chromatography; Coates, V. J.; Noebles, H. J.; Fagerson, I. S. Eds.; Academic Press, New York 1958.
6. Munk, P; Card, T. W.; Hattam, P.; El-Hibri, M. J.; Al-Saigh, Z.Y. Macromolecules 1987, 20, 1278.
7. Giddings, J. C. J. Chromatogr. 1961, 5, 49.
8. McQuarrie, M. J. J. Chem. Phys. 1963 38, 437.
9. Hattam, P.; Munk, P. Macromolecules 1988, 21, 2083.
10. McNally, M. E.; Grob, R. L. Amer. Lab. 1985, 17, 106.

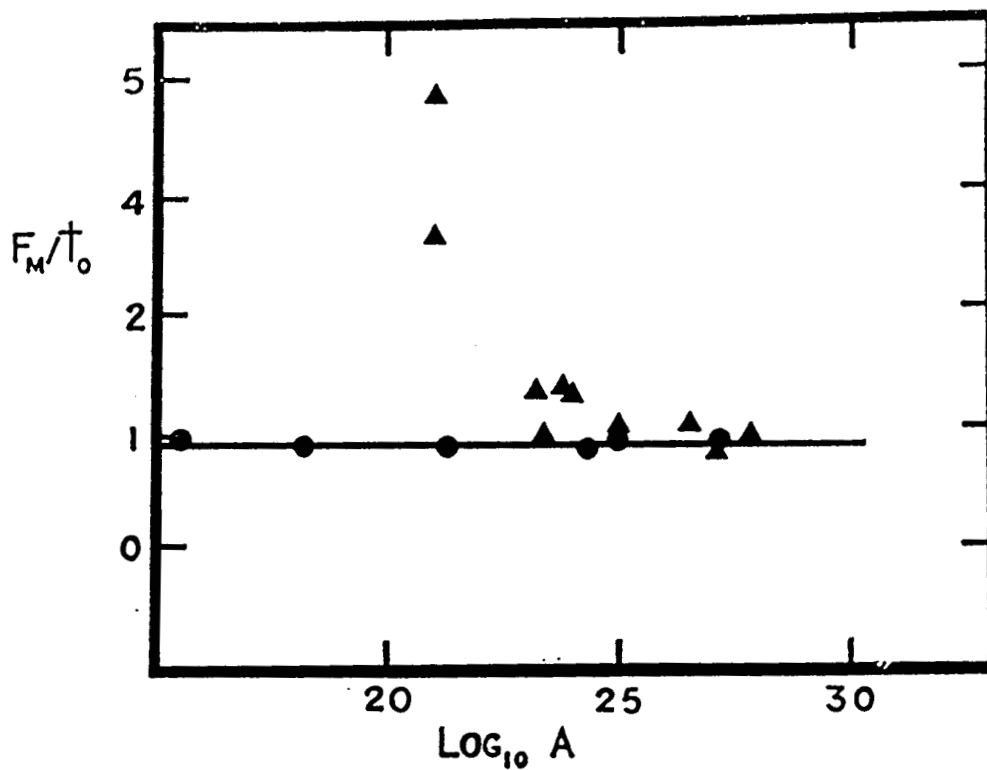


Figure 1. Dependence of  $t_R/t_0$  and  $F_M/t_0$  on  $\text{Log}_{10} M_{inj}$  for the simulation of surface adsorption.  $Z_g=0.002$ ;  $Z_p=0$ ;  $Z_s=1.0, 4.0, 10.0$ .

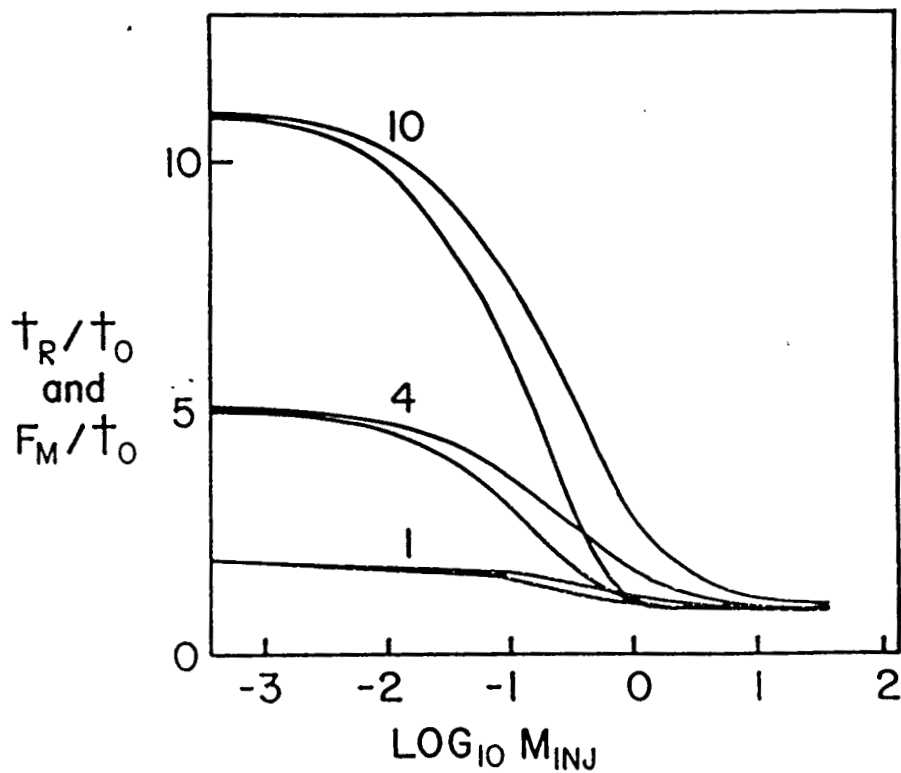


Figure 2. Dependence of the first moment on the amount of probe injected. ( $\blacktriangle$ ) probe injected as a liquid; ( $\bullet$ ) probe injected as a vapor.

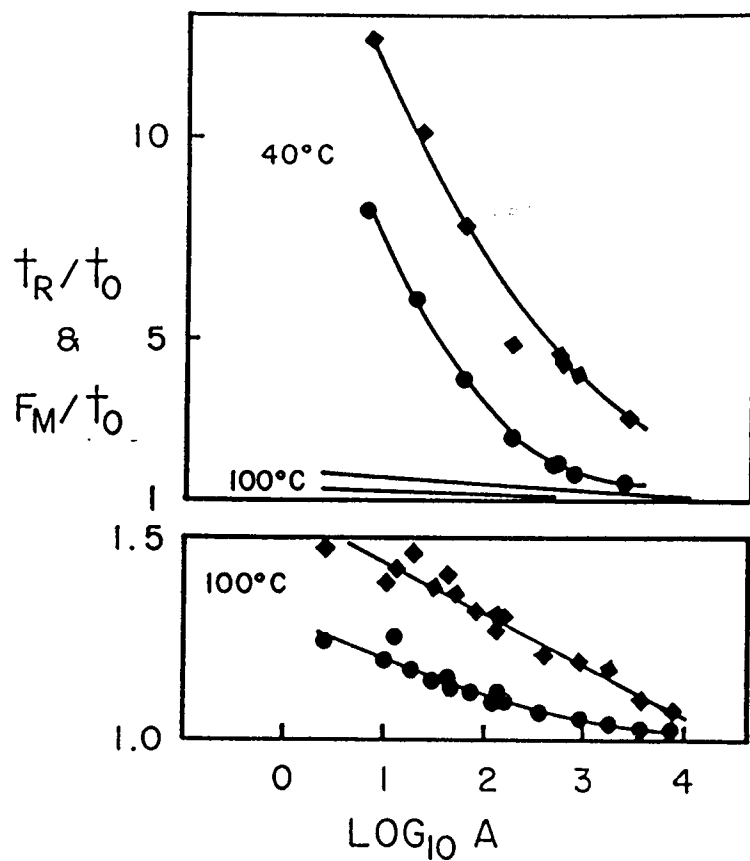


Figure 3. Dependence of  $t_R/t_0$  (●) and  $F_M/t_0$  (◆) on  $\text{Log}_{10} A$ , peak area, for acetone on an uncoated column at  $40^\circ\text{C}$  and  $100^\circ\text{C}$ . Data at  $100^\circ\text{C}$  plotted twice for comparison.